Investigation of Hydrogel Formation from Hydroxypropylmethylcellulose (HPMC) by NMR Spectroscopy and NMR Imaging Techniques

C. A. Fyfe* and A. I. Blazek

Department of Chemistry, University of British Columbia, 2036 Main Mall, Vancouver, BC, V6T 1Z1, Canada

Received January 22, 1997; Revised Manuscript Received June 28, 1997[⊗]

ABSTRACT: NMR imaging has been used to investigate the *in situ* swelling behavior of 2-hydroxypropylmethylcellulose (HPMC) tablets in a sample geometry chosen for the simplicity of its diffusion behavior. Preliminary ^{1}H NMR spectroscopy experiments were performed on equilibrated mixtures of HPMC and water. From these, the dependence of the ^{1}H T_1 and T_2 relaxation parameters of the water protons with respect to HPMC weight percent were obtained. Further analysis of the T_2 values and ^{1}H *z*-spectroscopic data revealed that as the polymer concentration was increased from 10% to 20% w/w HPMC, the polymer mobility decreased substantially. One-dimensional NMR imaging of ^{1}H in the swelling tablet system was used to monitor the movement of water into the polymer and to calculate the T_2 parameters across the system. HPMC weight percents were calculated from these T_2 values using the previously determined calibration. HPMC distributions were determined for two tablet thicknesses. Similar swelling behavior was observed for both thicknesses at early times prior to the thinner tablet becoming completely hydrated.

Introduction

Hydrogels are formed from hydrophilic polymers that swell when they absorb water. Although the penetrating water forces the polymer chains apart, the remaining physical entanglements maintain some "solid" characteristics for the swollen polymer. Thus, hydrogels behave as elastic solids and retain their shape. Many natural polymers such as gelatin, agar, and starch have the ability to form hydrogels. An industrially important class of hydrogel-forming polymers is cellulose derivatives such as methylcellulose and hydroxypropylmethylcellulose (HPMC) which are often employed as thickeners, emulsifiers, and adhesives in the food industry.[1] Many pharmaceutical tablets are also based on hydrophilic polymers. When exposed to water, the polymers form a gel layer around the tablet that limits the dissolution and diffusion of the drug and provides a mechanism for controlled drug release.[2]

The swelling behavior of these hydrophilic polymer tablets has been studied primarily by optical microscopy using polarized light and photography.[3−5] These experiments rely on the different optical properties of a dry and swollen polymer but may not be able to distinguish intermediate regions where water is present but not in sufficient quantities to change the optical properties. NMR imaging has been used to monitor the diffusion of solvents into synthetic polymers,[6,7] and some previous papers have used NMR imaging to track the penetration of water into swelling tablets.[8,9] However, these studies yielded only a qualitative description of the swelling process because the images were not acquired with parameters that guaranteed that the signal intensities throughout the images were directly related to water concentration and only the behavior of the water and not the polymer itself was investigated. In this paper we present results from a quantitative study using various NMR spectroscopic techniques combined with NMR imaging aimed at obtaining both insight into the nature of the water−polymer interactions and also a quantitative description of the kinetics and mechanism of the swelling process on the basis of the concentrations and mobilities of both water and polymer as functions of time and distance. It is hoped that in the future these latter data will serve as the basis for the design of imaging experiments to quantify the controlled release of intercalated drug molecules from swollen HPMC matrices.

Experimental Section

Materials. Hydroxypropylmethylcellulose (HPMC, Methocel K4M Premium) was obtained from DOW Chemical Co. and used as supplied. The moisture content of the starting powder was determined by thermogravimetric analysis (5.4%), and all weights and concentrations include corrections for moisture content. Various mixtures of HPMC and distilled water, ranging from 0% to about 60% HPMC by weight polymer over total weight, were prepared by mixing the appropriate amount of each component in a vial. The vials were then sealed, and the mixtures were allowed to equilibrate in a refrigerator. Tablets were prepared by direct compression of the as supplied "dry" HPMC powder using a rotary press. Two tablet thicknesses were prepared. The thin tablets weighed 162 ± 1 mg, were 12.75 ± 0.05 mm in diameter, and were 1.37 ± 0.01 mm thick. The peak compressional force for these tablets was 62 ± 3 MPa. The thick tablets weighed 323 ± 3 mg, were 12.75 ± 0.05 mm in diameter, and were 2.66 ± 0.01 mm thick. The peak compressional force for the thick tablets was 59.6 ± 0.9 MPa. The aspect ratios, i.e., the ratios of diameter to thickness, were 9.3:1 for the thin tablets and 4.8:1 for the thick tablets.

Measurements. The NMR spectroscopy and imaging experiments were carried out using a Bruker MSL400 (9.4 T) spectrometer with a Bruker microimaging probe incorporating a 15 mm vertical coil. The T_1 relaxation times of water (^{1}H) in the mixtures were determined at ambient temperature by an inversion-recovery sequence (180°−τ−90°-acquire) while the T_2 values were determined using a spin−echo sequence (90°−τ−180°−τ−acquire). Only one relaxation component was observed for the water signal in the equilibrated mixtures, even at the highest HPMC concentrations. Cross-relaxation or *z*-spectroscopy experiments were also performed for each of the HPMC/water mixtures.[10] In these, an off-resonance preparation pulse, with an excitation width of 500 Hz, was applied for 5 s before the spectrum of water was observed. The offset of the preparation pulse was varied from −100 to +100 kHz, and for a particular mixture, the intensity of the water

* Author to whom correspondence should be addressed.

[⊗] Abstract published in *Advance ACS Abstracts,* September 1, 1997.

S0024-9297(97)00076-4 CCC: $14.00

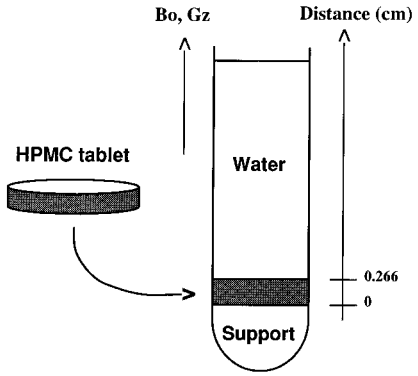

Figure 1. Tablet arrangement for the swelling experiment. The distance scale is measured from the face of the tablet resting against the support. The initial position for the water−tablet interface is 0.266 cm for the thick tablet (as shown) and 0.137 cm for the thin tablet.

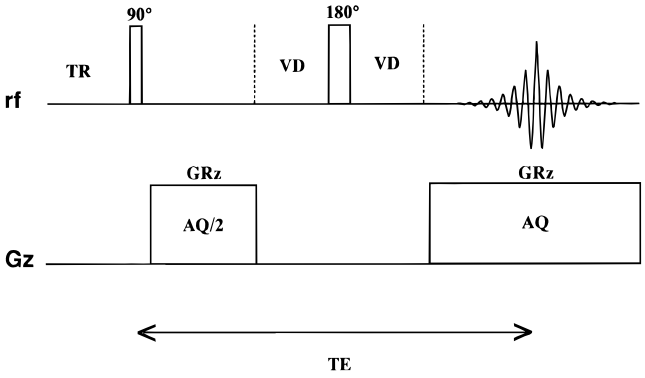

Figure 2. Pulse sequence used to acquire the one-dimensional projections. The variable experimental parameters are defined as follows: TR is the delay between successive experiments, 90° and 180° labels are radio frequency pulses, GRz is the strength of the *z*-gradient, AQ is the acquisition time, VD is a variable delay, and TE is the time-to-echo.

signal varied with the offset of this pulse. A plot of the normalized signal intensity versus the offset of the preparation pulse is referred to as the *z*-spectrum. A Doty Scientific microimaging probe was used to measure the self-diffusion coefficient of water in various mixtures by the pulsed−gradient spin−echo (PGSE) method.[11] The diffusion coefficient of water in 10 mM $CuSO_4$ solution, 2.35×10^{-5} cm^2 s^{-1}, was used to calibrate the gradients for the diffusion measurements.[11] The temperature for all of the experiments, as determined by a thermocouple and controlled by a variable temperature unit, was 22 ± 1 °C.

The swelling experiments were carried out with the tablet and water in a 15 mm NMR tube held vertically in the coil. The tablet was placed at the end of the tube as shown in Figure 1 with only one face of the tablet exposed to water. The bottom face and the edges of the tablet were sealed with a small amount of grease to prevent leakage of water between the tablet and the tube wall. The swelling experiment was initiated by adding 5 mL of distilled water to an initially dry tube containing the tablet. This quantity of water ensured a large enough excess that the swelling process could be considered semi-infinite. At different times, one-dimensional ^{1}H images were obtained along the axis of the tube using the spin−echo imaging sequence given in Figure 2. Using a gradient strength of 9.8 ± 0.2 G/cm, a spectral width of 83333.33 Hz, and a pixel number of 128, the resulting experimental field of view was just under 2 cm and the resolution in the images was 0.0156 cm. The repetition time (TR) was 20 s, five times the maximum T_1 value for water in the system. The time to echo (TE) in the spin−echo sequence was varied from 2 to 128 ms, in the order 2, 4, 16, 32, 96, 128, 64, 24, 8, and 3 ms, to observe the T_2 variation along the image. The acquisition time was about 3 min per image and about 30 min for the set of images. The data sets were acquired at 3 h intervals during an approximately 37 h experiment. The tablet-swelling experiment was repeated twice for the thin tablets and three times for the thick tablets.

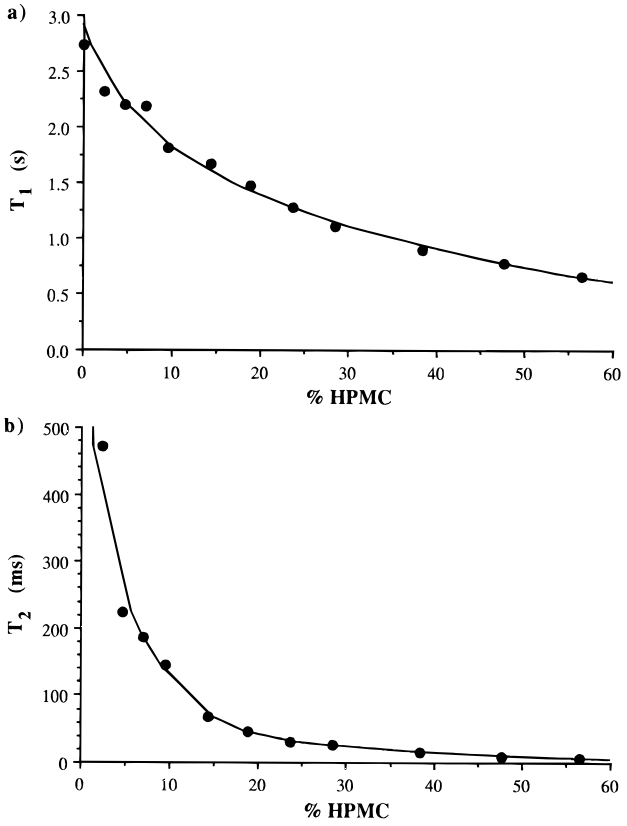

Figure 3. Variation of ^{1}H relaxation times of the water resonance in HPMC/water mixtures at equilibrium: (a) T_1 values and (b) T_2 values. The solid circles are the experimental points and the lines are the curves calculated using eqs 1 and 2, respectively.

Results and Discussion

NMR studies of hydrated HPMC itself and other polymers in the gel state are hampered by their broad spectral lines and short relaxation times. However, the characteristics of the polymer can be inferred indirectly through the influence of the polymer on other components in the system. Thus, the determination of the NMR properties of water in an HPMC environment leads to conclusions about the polymer itself and its behavior in the system.

^{1}H NMR Spectroscopic Investigation of HPMC/Water Mixtures at Equilibrium. NMR spectroscopy was used to measure how various parameters were affected by changes in the polymer concentration. The ^{1}H spin−lattice and spin−spin relaxation times, T_1 and T_2, respectively, were measured for the water resonances in equilibrated HPMC/water mixtures of varying polymer concentration. These relaxation times are dependent on the mobility of the water within the polymer matrix of the mixture. As expected, both T_1 and T_2 decreased as the weight percent of the HPMC increased (Figure 3), reflecting the decrease in the tumbling frequency of water in the mixtures due to the increase in the number of hydrogen-bonding interactions to the polymer chain hydroxyls. Equations 1 and 2, relating polymer weight percent and the T_1 and T_2 relaxation parameters, were obtained from nonlinear least squares fits of the data using the Mathematica program.[12] The curves calculated from the equations

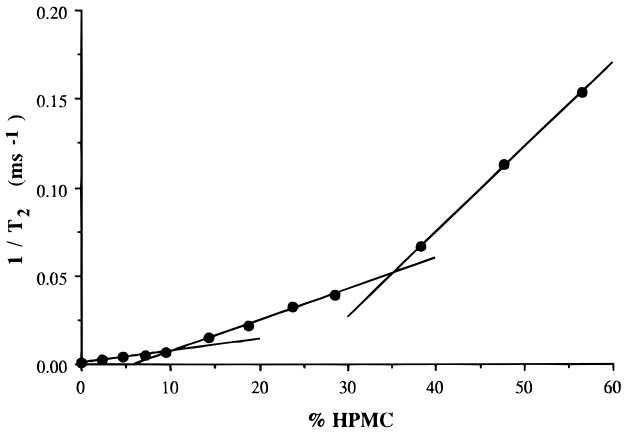

Figure 4. Plot of $1/T_2$ versus HPMC weight percent indicating discontinuities at ~12% and ~35% HPMC.

are overlaid with the data in Figure 3 and demonstrate that, in each case, the entire range of relaxation times could be smoothly described by a phenomenological equation. The T_1 data in Figure 3a show that the maximum T_1 value in the system is that of pure water. The repetition delay in future experiments was set to five times that of pure water to avoid discrimination of the NMR signals based on T_1 values. Equation 2 was used in a predictive manner, to calculate HPMC concentrations from the imaging experiments as discussed in the next section.

$$[\text{HPMC}] = 136.681 \exp(-1.274T_1) - 3.395 \quad (1)$$

$$[\text{HPMC}] = 54.86 \exp(-0.07119T_2) + 21.52 \exp(-0.006028T_2) \quad (2)$$

In the simplest description of the swollen polymer−water system, the water can be considered to exist in free and bound states. The fact that only one relaxation component is observed for the water nuclei indicates that these states are in rapid equilibrium relative to the NMR time scale. The free water has a longer T_2 value than the bound water, and the resulting average in the fast-exchange limit is a combination of the different T_2 values as shown in eq 3a where p_i is the fraction of water molecules in the ith state.[13] Assuming a single-bound state for the water, only two terms in eq 3a need be considered, yielding eq 3b. A plot of the inverse of the observed T_2 as a function of the fraction of bound water should yield a straight line with an intercept of $1/T_{2,\text{free}}$, in this case the inverse of the T_2 of distilled water.

$$\frac{1}{T_{2\text{obs}}} = \sum_i \frac{p_i}{T_{2i}} \quad (3a)$$

$$\frac{1}{T_{2,\text{obs}}} = \frac{p_{\text{free}}}{T_{2,\text{free}}} + \frac{p_{\text{bound}}}{T_{2,\text{bound}}} = \frac{1}{T_{2,\text{free}}} + p_{\text{bound}}\left\{\frac{1}{T_{2,\text{bound}}} - \frac{1}{T_{2,\text{free}}}\right\} \quad (3b)$$

For the various HPMC/water mixtures, the fraction of bound water is unknown but should be related to the concentration of the polymer. Figure 4 shows the plot of $1/T_{2,\text{obs}}$ versus HPMC weight percent. The data in Figure 4 appear to separate into three distinct linear regions. The data from 0% to 10% HPMC fall on one line, the data from 10% to 30% fall on a second line, and the values from 40% to 60% appear to fall on a third line. The slope for each line is $h\{1/T_{2,\text{bound}} - 1/T_{2,\text{free}}\}$ where the fraction of bound water is the product of the constant h and the weight percent HPMC. The intercept for the 0%−10% line yields $1/T_{2,\text{free}}$ as expected according to eq 3b, but the intercepts for the second and third lines are far removed from that value. There are two possible explanations for the discontinuities that occur at approximately 12% HPMC and 35% HPMC.[14] The hydration of the polymer may have changed, altering the bound water fraction and thus the coefficient h in the slope. Another explanation is that the T_2 of the bound water has changed. Since the T_2 of the bound water depends on the mobility of the polymer chain to which it is bound, a substantial change in the mobility of the polymer chain in the polymer/water mixture would cause a significant change in the $T_{2,\text{bound}}$. The first discontinuity in Figure 4 appears in the same, semidilute concentration region where the mixture would first be classified as a gel rather than as a viscous solution. The polymer chain in the gel state would be expected to be more restricted than in solution but more mobile than the solid polymer. Thus, the first discontinuity is probably due to a substantial decrease in chain mobility when the polymer becomes concentrated enough to form the physical entanglements required for the gel state. The second discontinuity occurs in the concentration region where the mixtures lose their transparency. The discontinuity at higher HPMC concentration may be due to dehydration to or below the water concentration necessary for optimum interchain, water-mediated H-bond cross-linking which would greatly restrict rotational motion of the chains.

In order to check this interpretation of the data of Figure 4, the mobility of the polymer component in the polymer/water mixtures was probed with cross-relaxation or *z*-spectroscopy. This experiment requires water to be in the presence of a polymer which provides so-called solid protons to interact with the bound water component. An off-resonance pulse, applied to saturate the resonances of the solid protons in the system, indirectly affects the magnetization of the water because, during the length of the pulse, cross-relaxation through dipolar coupling occurs between the protons of the bound water and those of the polymer. When the spectrum of the water is acquired after the off-resonance pulse, the intensity of the signal will decrease relative to the intensity in the absence of the preparation pulse, reflecting the fast-exchange process and the amount of cross-relaxation that has occurred. The *z*-spectrum is the plot of the normalized signal intensity, M/M_0, versus the offset of the presaturation pulse. Figure 5 shows the *z*-spectra for some of the HPMC/water mixtures. In general, the observation of these *z*-spectra provides direct evidence that substantial interaction occurs between the water and the polymer protons. Only water nuclei in close proximity to the polymer, i.e., bound water, can participate in cross-relaxation with the polymer protons because the magnitude of the dipolar coupling interaction is inversely proportional to the internuclear distance cubed. Exchange between the hydroxyls of the HPMC and the hydroxyls of the water would be an additional mechanism for magnetization transfer between the water and the polymer. The *z*-spectrum of distilled water is included to show the result of the same experiment on a sample where the possibility for cross-relaxation is absent. An important

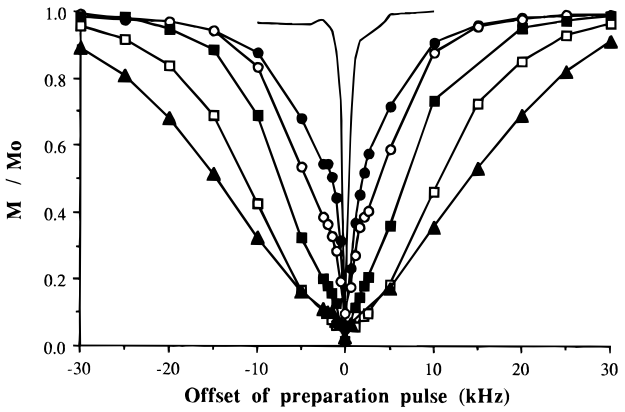

Figure 5. ^{1}H NMR *z*-spectra for selected HPMC/water mixtures from observation of the ^{1}H signal of H_2O (see text). The mixtures shown are water (solid line), 9.4% (●), 14.2% (○), 18.7% (■), 38.3% (□), and 56.6% (▲). A preparation pulse with an excitation width of 500 Hz was applied at different offset frequencies for 5 s prior to the acquisition of the water signal. (Only the range of offsets of −30 to +30 kHz is shown.)

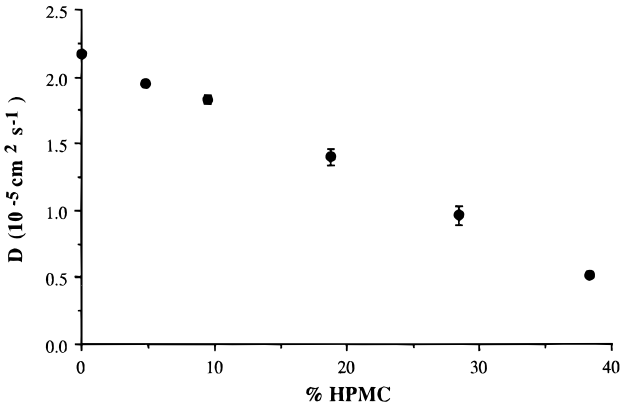

Figure 6. Self-diffusion coefficients of the water component in the HPMC/water mixtures as determined with the PGSE experiment.

feature of these plots is that the width-at-half-height of the *z*-spectrum is related to the width of the spectral line for the solid protons, even where, as in the present case, the proton spectrum of the solid component is not observed directly. The broad lines of solids are due to the presence of dipolar couplings that are not averaged to zero by motion. Thus, the less mobile the polymer chains, the broader the line for the polymer protons and the broader the corresponding *z*-spectrum for the water in the polymer. Figure 5 shows that the widths of the *z*-spectra increase with increasing polymer concentration. The width-at-half-height for the 20% mixture was almost five times that for the 10% mixture. No other doubling in polymer concentration resulted in such an increase in the width of the *z*-spectrum; the widths increased by about two times for all other comparisons. These results suggest that there is a very significant change in the mobility of the polymer when the polymer concentration passes between 10% and 20%. Thus, the results of the *z*-spectroscopy support the interpretation that the discontinuity at ∼12% in Figure 4 is the result of a change in the polymer mobility. Since there was not a correspondingly large change in the *z*-spectrum around 35% HPMC, the second discontinuity in Figure 4 is interpreted as a change in the hydration characteristics of the polymer.

The self-diffusion coefficients of the water components for each of the polymer/water mixtures were determined using the PGSE method. Figure 6 shows that the self-diffusion coefficient decreased slowly from 2.19×10^{-5} to 0.51×10^{-5} cm^2 s^{-1} as the weight percent of HPMC was increased from 0% to 40%. A range from 0.9×10^{-9} to 2.2×10^{-9} m^2 s^{-1} has been reported in the literature but it was unclear how these values related to the HPMC concentrations.[6] The gradual change of the diffusion coefficient with polymer concentration indicates that the mobility of the water in the mixtures decreased as the polymer concentration increased but was not significantly affected by the substantial change in the mobility of the polymer that occurs between certain polymer concentrations. The PGSE measurement determines the average displacement of the water molecules over a certain time which is affected by the fraction of time that the water is immobilized in the bound state. The average, however, depends on the amount of time spent in the bound state, but not necessarily on the nature of the state. Thus, the changes in the polymer mobility at certain concentrations were not evident in the measured water diffusion coefficients.

The changes in the polymer/water environment detected by NMR are reflected in the macroscopic behavior of the equilibrated mixtures. The dilute HPMC mixtures were transparent, viscous solutions. As the HPMC weight percent was increased past about 10% w/w, the mixtures became transparent gels until, at concentrations greater than 30% w/w, the HPMC/water mixtures became opaque rubbery materials. At concentrations of about 50% and 60%, the mixtures were coarse powders. Gradual changes in the T_2 values and the diffusion coefficient indicate that the mobilities of the water component do not change in any discontinuous way as the polymer concentration is changed in the equilibrium mixtures. The mobility of the polymer chain, however, decreased substantially as the polymer concentration was increased from 10% to 20% HPMC, i.e., the concentration region where gel behavior is first observed. The nature of the polymer−water interaction would be expected to be similar in the swelling tablet within volumes of polymer/water composition corresponding to those of the equilibrated test mixtures.

NMR Imaging Investigations of the Swelling of HPMC Tablets. In NMR imaging, the spatial information is encoded in the NMR signal by the use of magnetic field gradients in one or more of the *x*, *y*, and *z*-directions. The resulting image intensity is given by eq 4 where C is a constant, $\rho(H)$ the density of nuclear spins, TE and TR experimental delay times that can be varied in the spin−echo experiment (Figure 2), and T_1 and T_2 the relaxation times for the nuclei being imaged. To obtain the true spin density in the image, i.e., the true concentration of the molecular species being imaged, it is important to ensure that the second and third terms in eq 4 are as close to unity as possible by making TE $\ll T_2$ and TR $\gg T_1$ where the T_1 and T_2 values are known. Conversely, the dependence of the intensity on TE and TR can also be used to determine the T_2 (or T_1) relaxation times of a nucleus directly from a series of images obtained with different values of TE (or TR) with all other factors kept constant.

$$S(\mathrm{TE}) = C\rho(H)\exp(-\mathrm{TE}/T_2)(1 - \exp(-\mathrm{TR}/T_1)) \quad (4)$$

The experimental setup (Figure 1) was chosen to restrict the swelling of the tablet to one-dimension only, that of the axis of the tube. The cylindrical symmetry in the system allowed for a very simple and straight-

forward imaging study using a single gradient in the *z*-direction, perpendicular to the surface of the tablet. The advantage of the one-dimensional over the corresponding two-dimensional experiment is that, with the former, quantitative information about the system can be obtained in a reasonably short time which is an essential experimental requirement to properly monitor the changing distributions for water and polymer. This system is also a simple situation for quantitative measurements of diffusion with no loss of information. Two specific questions about the experimental setup need to be addressed. The first concerns the radial expansion of the tablet which is prevented in the experimental setup. It is possible that when the radial expansion of the tablet is restricted, additional pressures within the tablet will lead to an enhancement of the axial swelling. The thin HPMC tablets were prepared with a diameter-thickness ratio of about 10:1. With such dimensions, the thin tablets can be regarded as two-dimensional slabs, and contributions from radial effects can be ignored. The results of the swelling experiment for the thick tablet were comparable with that of the thin tablet even though the aspect ratio of the thick tablets was half that of the thin tablets. Thus, the radial effects seem to be minimal. The second question involves the assumption of uniform swelling across the tube, i.e., the absence of any boundary effects involving the tube walls. A two-dimensional imaging study of a swollen tablet, where a series of cross-sectional images were taken perpendicular to the axis of symmetry, confirmed that the intensity of the water signal was reasonably homogenous across the sample and that the assumption of cylindrical symmetry was valid.

One-dimensional water images were acquired for the swelling tablet system at regular intervals over an extended period of time to gain a full understanding of the water movement as the polymer swells. A large enough value was chosen for TR (20 s) to ensure complete recovery of water magnetization from all polymer regions and no dependence of the echo on T_1. At each interval, multiple images were acquired, and the length of TE in the pulse sequence was changed to obtain a map of the T_2 values in the system which were used to correct the intensity of the water signal for any loss due to dephasing during the shortest TE of 2 ms. The adjusted water images for both tablet sizes are shown in Figure 7. (The distances in this and following figures are measured from the face of the tablet that initially rested against the support at the bottom of the tube as indicated in Figure 1.) The intensity in these images is scaled relative to the signal intensity of the bulk water region. The water images display both the process of water penetration into the tablet, as is evident by the increase of signal in the originally dry tablet region, and the swelling of the polymer which results in a displacement of water and a loss of signal intensity in regions far away from the original tablet position. Small irregularities in the water signal are also visible which are caused by air bubbles, trapped during compression of the polymer powder and released during hydration. From the water images of Figure 7, the penetration distance of the active water front was measured. The penetration rates of water into the tablet are similar for both the thin and thick tablets which suggests that the thin tablet can be regarded as an outer layer of the thick tablet. Figure 8 shows a plot of the penetration distance into the tablet of the detectable, i.e., mobile, water as a function of the square root of time. The linearity of such a plot is the standard proof for a Fickian water diffusion process.[15]

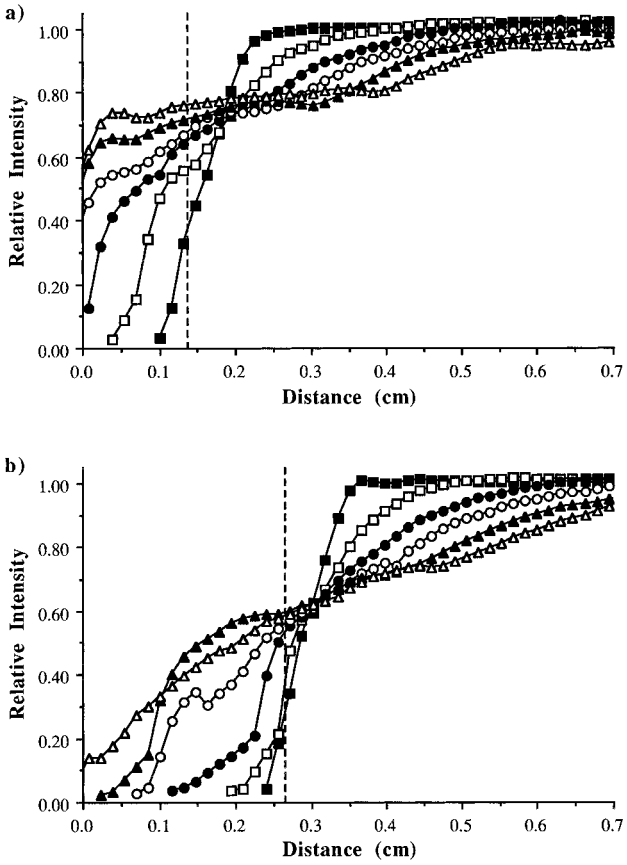

Figure 7. Time variation of the water projections: (a) thin tablet and (b) thick tablet. The intensities are scaled relative to the signal intensity of the bulk water region. The times are 1 h (■), 4 h (□), 10 h (●), 16 h (○), 25 h (▲) and 37 h (△). The dashed line indicates the original position of the water-tablet interface.

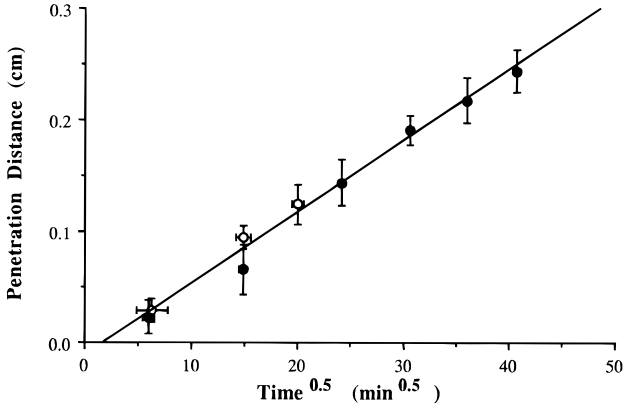

Figure 8. Average penetration distance of water into the thin (○) and thick (●) tablets as a function of the square root of time. The error bars in the distance are comparable to the error in determining the position of the zero from the imaging experiments. The slope and intercept of the line are 0.006415 and −0.01180, respectively.

The HPMC in the tablet was not imaged directly; however, as detailed in Figure 9, the polymer distribution can be calculated from water images acquired during the course of the swelling. Figure 9a shows the effect of TE on the signal intensity of water in the thin tablet at a swelling time of approximately 25 h. As TE was increased, the water signal from the concentrated

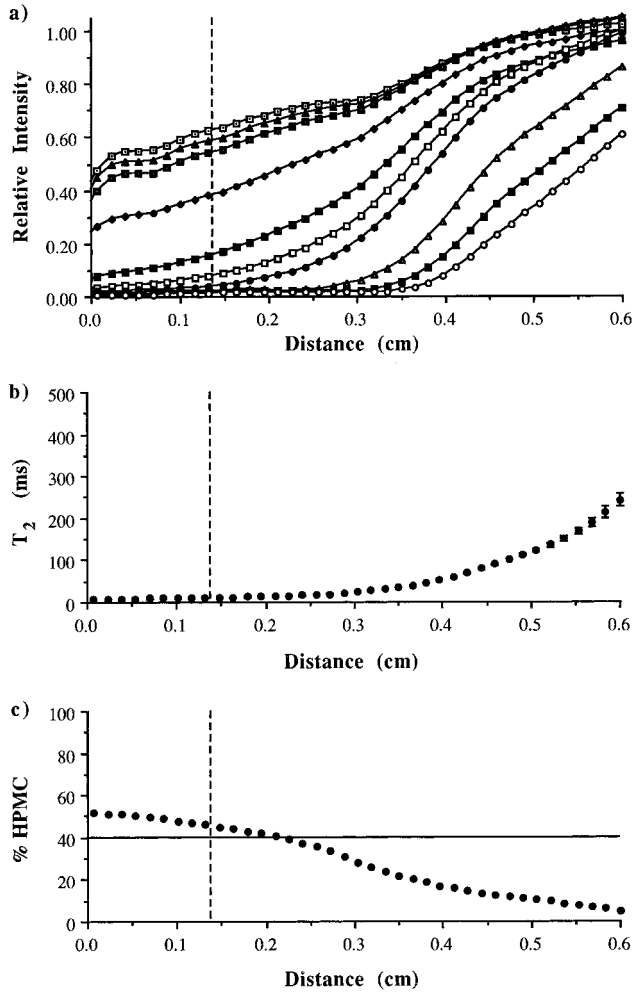

Figure 9. (a) Variation of the relative signal intensity from the water protons with TE in the spin−echo experiment for the thin tablet at a swelling time of approximately 25 h. The TE values, from top to bottom, are 2, 3, 4, 8, 16, 24, 32, 64, 96, and 128 ms, respectively. (b) Corresponding curve of T_2 values calculated from the slopes of plots of Ln(signal intensity) versus TE. (c) Polymer distribution in weight percent determined using eq 2. The vertical, dashed line in all three figures indicates the initial position of the water−tablet interface. The solid, horizontal line in (c) marks the upper limit for quantitative reliability of the HPMC weight percent.

polymer regions decreased rapidly because the T_2 values in that region are short in comparison to TE values. The T_2 value at a particular point is calculated from a plot of Ln(signal intensity) versus TE which has a slope of $-1/T_2$. The T_2 distribution, as shown in Figure 9b, is generated from such a plot for each point along the sample. The corresponding polymer distribution (Figure 9c) is obtained by converting the T_2 curve into HPMC weight percent using eq 2. The errors in the calculated weight percent should be largest at the higher concentrations because of the very limited dependence of T_2 on the HPMC weight percent between 40% and 60% HPMC (cf. Figure 3b). Because of this, the data corresponding to HPMC concentrations greater than 40% are considered to be only semiquantitative as indicated by the horizontal line in the figure.

A possible complication in the calculation of the HPMC distributions is the effect of water diffusion between pixels during the imaging sequence which would give lower apparent T_2 values and, thus, higher weight percents in the calculated HPMC distributions. Through detailed calculations,[16] it was determined that, with the present imaging parameters, there would be a ~30% decrease in the measured T_2 value for free water because of its fast diffusion. However, due to the combination of the lowering of the T_2 values of water below 200 ms (cf. Figure 3b) and the decrease of the water diffusion coefficient (cf. Figure 6), the effect of diffusion on the T_2 measurement was found to be much less significant for water contained within the swollen polymer tablet and negligible for the corresponding HPMC weight percents. For example, for the true T_2 values of 500, 200, and 100 ms, the corresponding HPMC weight percents are 1.1%, 6.5%, and 11.8%, respectively. When the diffusion of the water is taken into account, assuming the diffusion coefficient for free water, 2.3×10^{-5} cm^2 s^{-1}, and a TE of 128 ms, the calculations predict apparent T_2 values of 341, 169, and 91 ms, which correspond to HPMC weight percents of 2.8%, 7.8%, and 12.4%, respectively. Thus, the effect of diffusion between pixels leads to a worst-case increase of 1%−2% HPMC for each value. This increase was found to be acceptable within the errors of the imaging experiment. Therefore, the distributions presented here were not corrected for the effect of diffusion, although the correction would be straightforward as the diffusion coefficients are known for various polymer weight percents.

The resulting average HPMC distributions for both the thin and the thick tablets are presented in Figure 10. The times given in the caption are the median swelling times which take into account the 30 min experimental time required to obtain the complete data set needed to accurately calculate T_2. The initial polymer distributions of the thin and thick tablets are similar, supporting the view that, at early times, the thin tablet can be regarded as the outer layer of the thick tablet. At later times, once the thin tablet has become completely hydrated, the polymer distributions in the thin and thick tablet systems are no longer comparable. After 37 h of swelling, both tablets sizes quadrupled in thickness. In the equilibrated mixtures, gel characteristics were observed for polymer concentrations between 10% and 30% HPMC. It is assumed that in the swelling tablet, the same concentration distribution defines the gel layer of the polymer tablet. Thus, in Figure 8 regions that contain greater than about 30% HPMC remain essentially solid whereas in regions that contain less than 10% HPMC the polymer is slowly dissolving and diffusing into the bulk water.

Additional swelling experiments, not presented here, were performed to determine the possible effects of two factors, gravity and compression force, on the polymer distribution determined from the imaging experiment. The results presented in this paper are for systems where the polymer is swelling upward against gravity. In order to test for any effect due to gravity, the experimental setup was changed so that the tablet was resting with its top face against a support and the bottom face above a column of water. The edges of the tablet were sealed with a small amount of grease as for previous experiments to prevent water leakage between the tablet and the tube walls. In this system, the swelling occurred downward, and the polymer moved in the same direction as the force exerted by gravity. The water distributions and the polymer distributions calculated from the imaging experiments for swelling with gravity were the same as those measured and calculated for swelling against gravity. Thus, gravity had little or no effect on the polymer movement in these swelling systems.

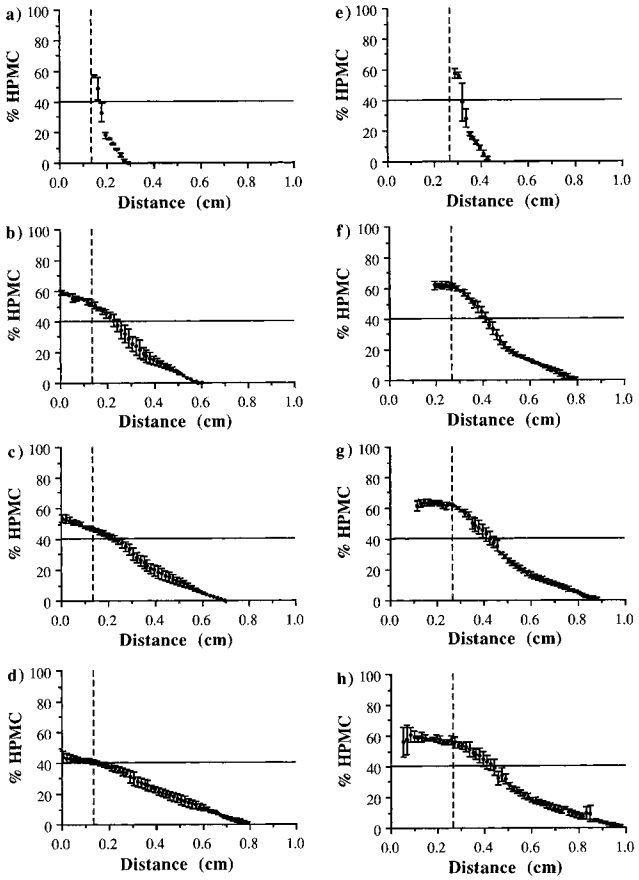

Figure 10. Average HPMC weight percent curves obtained from corresponding T_2 curves calculated from projections taken at different times-to-echo as in Figure 7. Figures (a)−(d) are the average of two experiments for the thin tablet and (e)−(h) are the average of three experiments for the thick tablet. The error bars represent standard deviations, and the dashed lines indicate the initial position of the water-exposed face of the dry tablet. The solid, horizontal lines in the figures mark the upper limit for quantitative reliability of the HPMC weight percent. Median swelling times are (a) and (e) 1 h, (b) and (f) 16 h, (c) and (g) 25 h, and (d) and (h) 37 h.

Swelling results for two 323 mg HPMC tablets prepared with different compression forces were also compared to determine if the compression force affected the water penetration and the polymer movement. One of the tablets, as in this paper, was compressed with a force of 60 MPa and had a thickness of 0.266 cm. The other tablet was compressed with a force of 105 MPa, resulting in a thickness of 0.246 cm. To compare the water penetration and polymer distribution results for these two tablets, the distance scale of the slightly thinner tablet was shifted by the difference in thickness so that the initial water−tablet interface was at the same position for each tablet. The water penetration and the calculated polymer distributions were similar for both tablets throughout the entire swelling. At the longer times of 30−37 h, there were small differences between the results for the two tablets due to the fact that the 0.246 cm tablet was completely penetrated by water at a slightly earlier time than the 0.266 cm tablet. The similarity between the two sets of results shows that the force of compression had little affect on the water penetration or the calculated polymer distributions for tablets of similar weight and thickness.

The ultimate goal of the present experiments was to use NMR imaging techniques to parametrize the expansion of the polymer tablet in terms of the polymer concentration as a function of both time and distance so that these data could be used in the future to test various possible models for the swelling process. Each data point in the polymer weight percent distributions in Figure 10 represents the amount of polymer in a certain volume region. If the volume and density are known, the weight percent profiles are easily converted into concentration units, such as grams per centimeters cubed, which better describe the amount of polymer at each location. To do this, the data must be corrected for the presence of air bubbles, otherwise the conversion from weight percent to grams per centimeters cubed would overestimate the amount of polymer present. It is worth noting that the presence of air has not been considered in most other investigations of swelling tablets where dimensional changes of the tablet were measured. Work on testing various possible models for the swelling is currently in progress and will be presented in a future publication when complete.

Qualitative Description of the Swelling Process. Some general features regarding the nature of the swelling process can be deduced from the data available for the polymer/water mixtures and from the swelling of the tablet itself. The changes in parameters that describe the mobility of water in the system lead to various conclusions about the polymer−water interaction. First, the water within the polymer exists in a rapid equilibrium between free and bound states as only a single relaxation component is observed. Second, there appeared to be no abrupt change in the mobility of water in the polymer/water mixtures, just a gradual decrease as the HPMC concentration was increased. Third, the polymer mobility underwent substantial changes when the concentration of the polymer passed into a region where gel behavior was observed.

The swelling of the polymer is attributed to the disruption of hydrogen bonding between polymer chains. When water penetrates the solid HPMC, it inserts itself into the hydrogen bonds between adjacent polymer chains. As more and more water comes between the chains, the forces between the chains diminish. The chains initially gain rotational freedom and begin to occupy more space which results in the swelling of the polymer mass. The penetrating water fills the voids between the polymer chains and diffuses into denser regions of polymer, forcing additional chains apart. Once the hydrogen bonds between chains are completely disrupted, a chain can disentangle and diffuse into the bulk water to become completely solvated. The swelling polymer can be approximated by three regions. The outermost region is composed of freely moving chains that are dissolving in the bulk water. The next layer in the tablet is the gel layer where there are still substantial cohesive forces between the chains. The innermost layer is composed of a polymer which has a low water content and is still primarily solid. The distinguishing properties between these layers are the hydration of the polymer and the subsequent mobility of the polymer chain.

Conclusions

The usefulness of NMR spectroscopy and NMR imaging techniques in the study of hydrogel swelling has been demonstrated. The investigation of the NMR characteristics of water in the HPMC environment makes possible the determination of relative polymer mobility and the calculation of the polymer distribution in the swelling process. Future work will concentrate

on the development and analysis of a model to describe the polymer swelling behavior on the basis of distributions obtained from these NMR imaging studies.

Acknowledgment. The authors acknowledge the financial assistance of the NSERC of Canada. A.I.B. acknowledges the award of an NSERC PGS Fellowship and an I. W. Killam Predoctoral Fellowship. The authors also thank the UpJohn-Pharmacia company for the gift of the HPMC used in this study and Dr. R. Miller and R. Oates of the Department of Pharmaceutical Science, UBC, for their help in the use of a rotary tablet press. Dr. B. Fahie, Glaxo-Wellcome Canada, and Dr. P. Gao, UpJohn-Pharmacia, are thanked for helpful discussions.

References and Notes

(1) Glicksman, M. In *Food Hydrocolloids*; Martin Glicksman, Ed.; CRC Press: Boca Raton, FL, 1982; Vol. 1. Chapter 1.
(2) Alderman, D. A. *Int. J. Pharm. Technol. & Prod. Manuf.* **1984**, *5*, 1−9.
(3) Thu Pham, A.; Lee, P. I. *Pharm. Res.* **1994**, *11*, 1379.
(4) Korsmeyer, R. W.; Gurny, R.; Doelker, E.; Buri, P.; Peppas, N. A. *Int. J. Pharm.* **1983**, *15*, 25.
(5) Gao, P.; Meury, R. H. *J. Pharm. Sci.* **1996**, *85*, 725−731.
(6) (a) Rothwell, W. P.; Holeck, P. R.; Kershaw, J. A. *J. Polym. Sci., Polym. Lett. Ed.* **1984**, *22*, 241. (b) Rothwell, W. P.; Tutunjian, P. N.; Vinegar, H. J. In *New Directions in Chemical Analysis*, Proceedings of the Third Symposium of the Industry-University Cooperative Chemistry Program of the Department of Chemistry, Texas A&M University, 1985; Shapiro, Bernard L., Ed.; Texas A&M University: Texas, 1985; pp 366−395. (c) Blackband, S.; Mansfield, P. *J. Phys. C.: Solid State Phys.* **1986**, *19*, L49. (d) Weisenberger, L. A.; Koenig, J. L. *Appl. Spectrosc.* **1989**, *42*, 1117.
(7) Fyfe, C. A.; Randall, L. H.; Burlinson, N. E. *J Polym. Sci.: Polym. Chem.* **1993**, *31*, 159−168.
(8) (a) Rajabi-Siahboomi, A. R.; Bowtell, R. W.; Mansfield, P.; Davies, M. C.; Melia, C. D. *Pharm. Res.* **1996**, *13*, 376. (b) Rajabi-Siahboomi, A. R.; Bowtell, R. W.; Mansfield, P.; Henderson, A.; Davies, M. C.; Melia, C. D. *J. Controlled Release* **1994**, *31*, 121. (c) Bowtell, R.; Sharp, J. C.; Peters, A.; Mansfield, P.; Rajabi-Siahboomi, A. R.; Davies, M. C.; Melia, C. D. *Magn. Reson. Imaging* **1994**, *12*, 361.
(9) Ashraf, M.; Iuorno, V. L.; Coffin-Beach, D.; Evans, C. A.; Augsburger, L. L. *Pharm. Res.* **1994**, *11*, 733.
(10) Grad, J.; Bryant, R. G. *J. Magn. Reson.* **1990**, *90*, 1.
(11) Stejskal, E. O.; Tanner, J. E. *J. Chem. Phys.* **1963**, *42*, 288.
(12) Wolfram Research, Champaign, IL, Guide to Standard Mathematica Packages. Technical Report Version 2.1, 1992; p 331.
(13) Zimmerman, J. R.; Britten, W. E. *J. Phys. Chem.* **1957**, *61*, 1328.
(14) Derbyshire, W. In *Water: A Comprehensive Treatise*; Franks, Felix, Ed.; Plenum Press: New York, London, 1982; Vol. 7, Chapter 4.
(15) Gehrke, S. H.; Biren, D.; Hopkins, J. J. *J. Biomater. Sci., Polym. Ed.* **1994**, *6*, 375.
(16) Brandl, M.; Haase, A. *J. Magn. Reson. Ser. B* **1994**, *103*, 162−167.

MA970076O